

Nonlinear effects in bismuth under cyclotron-resonance conditions

V. F. Gantmakher, G. I. Leviev, and M. R. Trunin

Institute of Solid State Physics, USSR Academy of Sciences

(Submitted 6 November 1981)

Zh. Eksp. Teor. Fiz. 82, 1607-1616 (May 1982)

The high-frequency properties of bismuth are investigated as functions of the magnetic field H in the cyclotron-resonance region in a wide range of the incident-wave frequency ω . The nonlinear-reflection signal at the second-harmonic frequency 2ω was registered in the experiment. Both cyclotron resonances, defined by the usual condition $\omega = n\Omega$ ($\Omega = eH/mc$, $n = 1, 2, 3, \dots$), in the form of spikes of the generated signal, and resonances of the type $2\omega = n'/\Omega$ ($n' = 1, 2, 3, \dots$), in the form of radiation dips, were observed in this signal. An additional structure can be seen in the intervals between the resonances. With increasing incident-wave amplitude, the resonance lines are inverted and broaden. A qualitative model, based on the ineffectiveness concept and demonstrating the onset of resonances of both types, is presented.

PACS numbers: 76.40. + b

INTRODUCTION

When an electromagnetic wave with frequency ω of sufficiently large amplitude is incident on the surface of a metal, a wave of double the frequency 2Ω is generated in the skin layer of the metal because of the nonlinear properties of the electron-hole plasma. Under conditions of anomalous skin effect, the amplitude A and the phase φ of this wave depend on the relations between the spatial and temporal parameters of the electron trajectories (the Larmor radius R , cyclotron frequency Ω , and others), on the one hand, and on the corresponding parameters of the wave in the skin layer (the depth δ , the frequency ω) on the other. In particular, as reported in Ref. 1, cyclotron resonances can be observed in the dependence of the amplitude of the generated wave on the magnetic field. Besides the resonances defined by the usual conditions

$$\Omega_n = \omega/n, \quad \Omega = eH/mc, \quad n=1, 2, 3, \dots \quad (1)$$

(we shall call them integer resonances), there were observed in Ref. 1 also resonances of the type

$$\Omega_{n'/2} = 2\omega/n', \quad n'=1, 2, 3, \dots \quad (2)$$

which are due to satisfaction of the resonance conditions at the doubled frequency (half-integer resonances). At even n' , the half-integer resonances (2) are superimposed on the integer resonances (1) with $n = n'/2$.

The existence of nonlinear cyclotron resonance was indicated in a cycle of theoretical papers²⁻⁴ dealing with nonlinear reflection of an electromagnetic wave of frequency 2Ω from a metal in a magnetic field parallel to the surface in the case of the anomalous skin effect.

Reference 1 was preliminary in character and left a number of questions unanswered. In particular, the resonance lines were too broad and the positions of their maxima did not agree very well with the calculated values. At the same time, the results of the theoretical calculations²⁻⁴ turned out to be extremely sensitive to the boundary conditions on the metal surface and to bulk scattering. These circumstances

stimulated further experimental investigations of the nonlinear cyclotron resonance in bismuth.

We report here the results of an experimental investigation of second-harmonic generation in the region of cyclotron resonance in bismuth on samples of two orientations (normal to the surface $n \parallel C_3$ and $n \parallel C_2$) in a wide range of incident-wave amplitudes. It turned out that the dependence of the amplitude of the signal on the magnetic field was determined not only, and not even so much, by the state of the surface as by the amplitude of the incident wave.

PROCEDURE

The experiment consisted of irradiating a bismuth sample by an electromagnetic wave of high frequency $\omega/2\pi = 9.3$ GHz, and detecting a signal of frequency of 2ω in the sample.

The sample 1 (Fig. 1) in the form of a disk of 17.8 mm diameter was placed at the bottom of a bimodal cylindrical resonator 2 operating on the E_{010} mode at a frequency 9.3 GHz and on the H_{111} at double that frequency. The sample was electrically insulated from the resonator by a paper liner 3.

The resonator was excited by a pulsed magnetron with pulse duration 2 μ sec at a repetition frequency 40 Hz. The radiation spectrum of the magnetron M contained many harmonics that could serve as sources of a false signal. To protect against harmonics from the magnetron, a system of absorbing filters F was used. The attenuator A_1 was used to vary the wave power absorbed in the resonator from 0.1 to 400 W; at a resonator Q equal to 2000, this corresponds to a maximum amplitude 0.5 to 30 Oe of the high-frequency fields at the sample.

Radiation of fundamental frequency ω was applied to the input of the resonator through 23×10 mm waveguide 4 through a slit S_ω . The 2ω harmonic was extracted through slit $S_{2\omega}$ through waveguide 5 of cross section 11×5.5 mm, so that the fundamental-frequency radiation could not enter the receiver. The received signal was fed through attenuator A_4 to a superheterodyne receiver

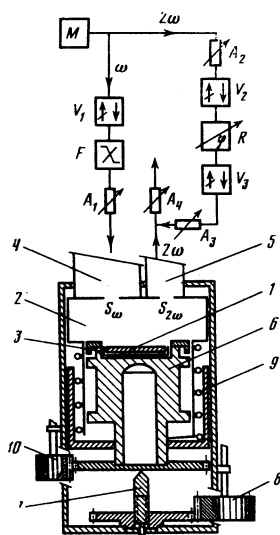


FIG. 1. Block diagram of high-frequency channels and construction of the bimodal resonator.

and then through a peak voltmeter to the y -input of an x - y recorder. The quantity measured was the power $P_{2\omega}$ of the radiated wave of frequency 2ω , i.e., a quantity proportional to the square of the amplitude $E_{2\omega}$ of the doubled-frequency electric field at the surface of the metal:

$$P_{2\omega}(H) \sim |E_{2\omega}(H)|^2. \quad (3)$$

In practice, the receiving system operated in the regime (3) only when the received signal reached a certain finite value. It was therefore convenient to investigate weak signals by applying a microwave bias to the detector. In this case the second harmonic was first separated from the magnetron spectrum and was used as the reference wave. It was fed through a channel containing the attenuators A_2 and A_3 , the rectifiers V_2 and V_3 , and the phase shifter R to the receiving system, where this reference signal of amplitude E_{ref} was mixed with the received signal $E_{2\omega}$. Inasmuch as only the dependences of $E_{2\omega}$ on the magnetic field are of importance in experiment, the quantity recorded by the plotter under the condition $|E_{ref}| \gg |E_{2\omega}(H)|$ is

$$A_{2\omega}(H) \approx |2E_{ref}E_{2\omega}(H)| \sim |E_{2\omega}(H)|. \quad (4)$$

The presence of a phase shifter in the reference-signal channel made it possible to measure the variation of the phase of the wave generated in the sample as a function of H .

The resonator was tuned in the following manner. A klystron (not shown in Fig. 1) was used first to determine the natural frequency ω of the resonator at the E_{010} mode. Next, moving the piston 6 with the aid of the rod 7 and the gear 8, the corresponding frequency of the resonator in the H_{111} mode was tuned to the value 2ω . Since the frequency of the E_{010} mode depends very little on the height of the resonator, exact matching of the frequencies could be attained by repeating this procedure 2 or 3 times (the absence of backlash was ensured by spring 9). The last stage consisted of tuning the magnetron to the frequency ω . The gear 10 made it

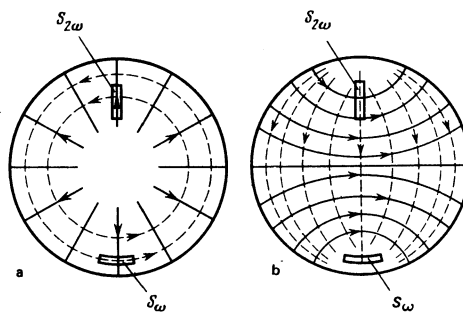


FIG. 2. Configuration of the fields in the resonator at the frequencies ω (a) and 2ω (b) (the solid and dashed lines represent the electric and magnetic field, respectively); S_ω and $S_{2\omega}$ are slits that couple the resonator with the waveguides.

possible to rotate the sample of the resonator directly during the time of the helium experiment.

Liquid helium flowing around the sample kept it from overheating. Special experiments have verified that decreasing the magnetron-pulse duration by a factor of 50 does not change the observed picture. At the same time, a change in the bath temperature by several tenths of a degree can be revealed by the changes in the shapes of the curves. All the results cited in this article were obtained by $T = 1.5$ K.

The magnetic field was produced by a Helmholtz system. The magnetic field could be rotated in the plane of the sample surface through any angle, and also inclined $\pm 5^\circ$ to the surface. The earth's field was cancelled out beforehand with approximate accuracy 2-3%.

Figure 2 shows the configuration of the electric and magnetic fields of both modes at the sample located in the resonator. The amplitude of the magnetic field at the frequency ω is zero at the center and on the wall, so that it reaches a maximum H_ω at a distance 9 mm from the center. The signal from the receiving waveguide came only from that resonator 2ω component whose currents were perpendicular to the slit $S_{2\omega}$, i.e., only the field of the mode shown in Fig. 2 was registered.

Most experiments described in the present article were performed on samples with the normal $\mathbf{n} \parallel C_3$. The samples were always mounted such that the C_2 axis was directed along the slit $S_{2\omega}$ (see Fig. 3; the accuracy of the setting was monitored by the symmetry of the effect and could reach $10'$). The currents produced by the electrons of the ellipsoid α did not participate therefore in the formation of the registered mode.

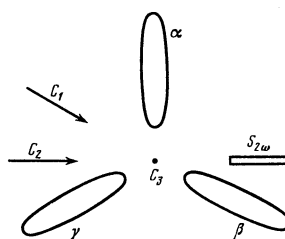


FIG. 3. Arrangement of the electron ellipsoids in samples with $\mathbf{n} \parallel C_3$ relative to the high-frequency field.

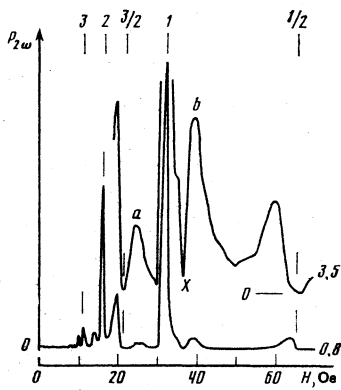


FIG. 4. Typical plot of $P_{2\omega}(H)$ for the sample with $\mathbf{n} \parallel C_3$ and $\mathbf{H} \parallel C_2$; the null level $P_{2\omega}=0$ equals zero and the maximum field amplitude H_{ω} in oersteds are marked on each curve (the numbers on the left); $P_{2\omega}$ is an arbitrary units.

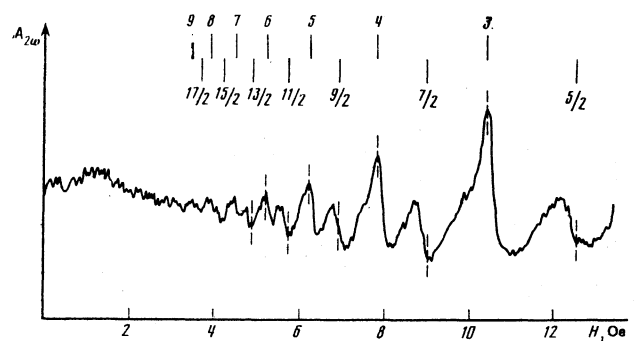


FIG. 5. Cyclotron resonances with large indices in radiation of doubled frequency for the sample with $\mathbf{n} \parallel C_3$ and $\mathbf{H} \parallel C_2$; $A_{2\omega}$ is in arbitrary units.

At \mathbf{H} parallel to the slit (the C_2 direction), the ellipsoid β and γ produced resonances in the same fields. With the magnetic field along the vector C_1 , the resonant fields from the ellipsoid β were half as strong as from the ellipsoid γ .

Altogether, investigations were made on seven samples with thickness from 0.6 to 2 mm.

RESULTS

Figure 4 shows a typical plot of the signal at the doubled frequency as a function of the magnetic field H directed along the C_2 axis (C_2 direction in Fig. 3), when the ellipsoids β and γ are equivalent. The vertical lines mark the values (1) and (2) of the resonant fields, calculated from the known values of the cyclotron masses.⁵

The most intense second-harmonic generation takes place in fields corresponding to integer resonances (1). On the lower plot of Fig. 4 one can see three such resonances with indices 1, 2, and 3. The width of the resonance with $n=1$ is approximately $\Delta H/H \approx 2\%$. In the gaps between the integer resonances (1) there is also radiation that depends nonmonotonically on the magnetic field. One can see clearly against the background of this radiation the resonances (2) with half-integer indices, which take the form of abrupt dips.

Phase measurements have shown that on passing through the resonances the phase of the signal changes by approximately 2π . Despite the difference in the line shape, rapid changes in the signal phase occur in either type of resonance only near the resonant value of the field. This gives grounds for stating that the broad maximum to the left of the half-integer resonances is outside the resonance line proper. This is also clearly seen in the plots obtained with the reference signal.

As seen from Fig. 5, the resonance lines retain the same shape also for resonances of high order with large n and n' .

Besides the half-integer resonances, the background signal contains also an additional structure. When the magnetic field is rotated the position of this structure

on the magnetic-field scale shifts together with the resonance lines. This seems to indicate that the background signal is formed mainly by bulk electrons that do not collide with the sample surface. The broad maximum on the left of the half-integer resonances is one example of such a structure, others being the maxima a and b of Fig. 4, which are satellites of the resonance $n=1$. Inasmuch as the relative width of the resonances increases with increasing number, it is difficult to say whether these satellites are duplicated near resonances in weak fields.

On the upper curve of Fig. 4, against the background of the satellite b , we can see clearly a narrow minimum X . When the magnetic field is rotated relative to the C_2 axis and the two ellipsoids become nonequivalent, this minimum splits just as the resonant maximum.

Notwithstanding the detailed investigations of the cyclotron resonance in Bi in the linear regime,⁵ the elaborate additional structure on the curves of Fig. 4 has made it desirable to perform a supplementary experiment—measurement of the impedance with the same setup and under the same conditions. Figure 6 shows the magnetic-field dependence of the signal U proportional to the change of the power of the wave of frequency 2ω passing through the resonator. (The signal from the klystron was fed to the resonator through the channel A_2-A_3 , see Fig. 1; the reflected signal passed through the broad waveguide 4 directly to the detector, and from it to the y -input of the plotter.) This signal is proportional to a linear combination of small changes of the real and imaginary parts of the impedance $U = \alpha \Delta R + \beta \Delta X$. On the $U(H)$ curve one can see the

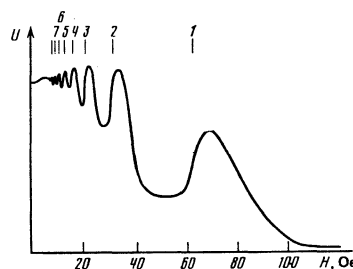


FIG. 6. Variation of the power of a wave of frequency 18.6 GHz passing through the resonator in the linear regime, as a function of the magnetic field (arbitrary units).

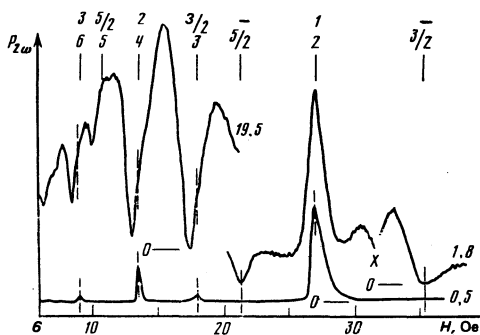


FIG. 7. Plot of $P_{2\omega}(H)$ for the sample with $\mathbf{n} \parallel C_3$ and $\mathbf{H} \parallel C_1$. The values of H_ω are indicated on the right of the curves. The upper and lower rows of indices pertain to resonances from the ellipsoids β and γ respectively.

cyclotron resonances clearly, and there is no additional structure whatever.

The indicated features of the shapes of the resonances are preserved also at $\mathbf{H} \parallel C_1$ (the two lower curves of Fig. 7), although the picture here is more complicated because of the difference between the cyclotron masses of the ellipsoids β and γ . There is also a minimum X near the integer resonance $n_\beta = 1$.

For the sample with the other direction of the normal, $\mathbf{n} \parallel C_2$, the shape of the $P_{2\omega}(H)$ curve near half-integer resonances was exactly the same as in Figs. 4, 7, and 8.

Usually the wave amplitude $A_{2\omega}$ at the doubled frequency is proportional to the square of the field at the fundamental frequency^{6,7}

$$A_{2\omega} \propto A_\omega^2. \quad (5)$$

This implies that the perturbation theory can be used to describe the frequency conversion. All the results discussed so far pertain to the interval of amplitudes A_ω in which (5) is valid. It was easy, however, to go outside the region (5) in the described experiments. In this case the deviation from the square law sets in at much smaller amplitudes in the field of an integer resonance than outside the field (see Fig. 9). In addition, the larger the index of the resonance, i.e., the weaker

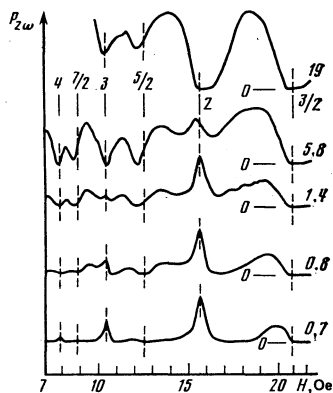


FIG. 8. Inversion of resonance lines with increasing H_ω . The values of H_ω are marked on the right of the curves. The sensitivities differ for the different curves; $\mathbf{n} \parallel C_3$, $\mathbf{H} \parallel C_2$.

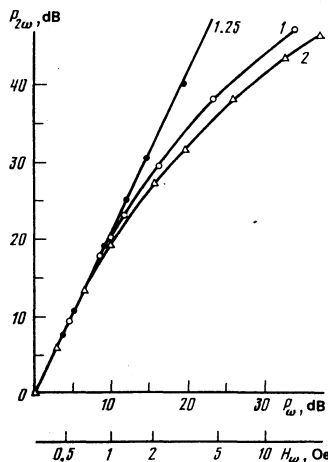


FIG. 9. Dependence of the radiated power $P_{2\omega}$ on the power P_ω incident on the sample in different magnetic fields, $\mathbf{n} \parallel C_3$, $\mathbf{H} \parallel C_2$. The numbers at the curves indicate a ratio H_1/H where $H_1 = 31.5$ Oe is the field of the integer resonance $n = 1$.

its fields, the sooner the deviation sets in. Saturation of the resonant signal is accompanied by broadening of the resonance line.

The result of saturation of the resonant signal is inversion of the cyclotron resonance lines (see Figs. 7 and 8). The inversion sets in sooner the weaker the field in which the resonance is located. It is typical that even after the inversion has occurred, pronounced resonance lines are preserved, although they are broadened and shifted towards weaker fields. This is seen particularly clearly on the upper curve of Fig. 7.

We note in this connection that the experimental curve given in Ref. 1 corresponds to intermediate amplitudes H_ω , when some of the resonances have already been inverted.

DISCUSSION

The appearance of a signal at the doubled frequency can be described in the following manner. Owing to the nonlinear properties of the medium, a component $j_{2\omega}^{(0)}(z)$ at the doubled frequency 2ω appears in the current induced by the incident large-amplitude wave. This component plays the role of an extraneous current, i.e., of an external source that excites in the metal the electromagnetic field at double the frequency. The value of this field, as well as the value of the total current $j_{2\omega}(z)$ flowing in the metal, depends on the linear conductivity $\sigma_{2\omega}$ at the doubled frequency:

$$j_{2\omega}(z, H) = j_{2\omega}^{(0)}(z, H) + \hat{\sigma}_{2\omega}(H) E_{2\omega}, \quad (6)$$

where the linear conductivity $\hat{\sigma}_{2\omega}$, generally speaking, can be also nonlocal. Since the amplitude of the wave radiated into the vacuum is determined by the field $E_{2\omega}$, it is seen from (6) that the cause of the nonmonotonic $P_{2\omega}(H)$ dependence observed in the experiment can be $j_{2\omega}^{(0)}$ as well as $\hat{\sigma}_{2\omega}$.

For a rigorous calculation of $j_{2\omega}^{(0)}(z)$ it is necessary to solve the kinetic equation, in analogy with the procedure used in Refs. 3 and 4. We confine ourselves here

to qualitative but intuitive arguments based on the ineffectiveness concept,⁸ with account taken of one of the possible nonlinearity mechanisms, namely, the influence of the magnetic field of the wave on the parameters of the electron trajectories in an external magnetic field. It is known that at low frequencies this influence leads to a number of nonlinear effects.⁹ In contrast to Ref. 9, we shall take into account the influence of the field of the wave not on the dimension of the orbit but on the period of revolution in it.

In analogy with Ref. 10, we express the current j induced in the metal in terms of the number N_{eff} of the effective electrons and of their effective range l_{eff} :

$$j = E \sigma_{\text{eff}} = E \sigma_0 \frac{N_{\text{eff}} l_{\text{eff}}}{N_0 l} = E \sigma_0 e^{i\omega t} \frac{\delta}{l} \sum_{p=0}^{\infty} e^{i\omega t_p}, \quad (7)$$

where $E = E_0 e^{i\omega t}$ is the electric field of the external wave, $\sigma_0 = N_0 e^2 l / p_f$ is the static conductivity, l is the mean free path, and the quantities t_p take into account the change of the phase of the wave in the p th return to the skin layer and the probability ν of scattering in the volume, $\nu \ll \omega$.

$$t_p = p \left(T + \frac{i}{\nu} \right) + \sum_{m=1}^p \tau_m, \quad T = \frac{2\pi}{\Omega}, \quad p \geq 1,$$

where τ_m is the change, due to the wave field H_ω which we assume directed parallel to the external field H , in the time of flight through the skin layer:

$$\tau_m = \alpha \cos[\omega(mT + t)], \quad \alpha = T(\delta/R)^{1/2} (H_\omega/H) \quad (8)$$

(numerical factors of the order of unity have been left out of α).

Let the wave amplitude H_m be not too large, so that the inequality

$$p\omega\alpha \ll 1 \quad (9)$$

holds. Since the terms of importance in (7) are those with $p \lesssim \Omega/\nu$, and this relation determines the relative width $\Delta H/H \approx \nu/\Omega$ of the resonance line, the inequality (9) reduces to

$$H_m \ll n^{-1} (R/\delta)^{1/2} \Delta H, \quad n = \omega/\Omega. \quad (10)$$

The inequality (9) allows us to expand

$$\exp\left(i\omega \sum_1^p \tau_m\right)$$

in (7) in a series and confine ourselves to the term linear in α . Summing (7) and separating from it the term proportional to $\exp(i2\omega t)$, we obtain

$$j_{2\omega}^{(0)} = E_0 \sigma_0 e^{i2\omega t} \frac{\delta}{l} \omega \alpha \frac{e^{w_s}}{(1-e^{w_s})(1-e^{w_s})}, \quad w_s = (i\omega - \nu)T, \quad s=1,2. \quad (11)$$

Thus, the extraneous current (11) contains resonant factors in the denominator for both integer (1) and half-integer (2) resonances, but the singularities in the integer resonances are stronger, since for these resonances both quantities in the parentheses in the denominator reach the minimum value ν/Ω simultaneously.

As for the conductivity $\hat{\sigma}_{2\omega}(H)$, we can formulate the following statement. A resonant conductivity increase of any origin (cyclotron resonance, paramagnetic resonance, etc.) decreases the radiation $P_{2\omega}$ from the metal

because of the additional energy dissipation at the frequency 2ω in the resonating system. In particular, such a resonating system can be those very electrons that generate the current (11). For these electrons the linear conductivity $\sigma_{2\omega}$, according to Ref. 10, is given by

$$\sigma_{2\omega} = \sigma_0 \frac{\delta}{l} (1 - e^{w_s})^{-1}. \quad (12)$$

If we now solve, in the ineffectiveness-concept approximation, Maxwell's equations with $j_{2\omega}^{(0)}$ in the form (11) and $\sigma_{2\omega}$ in the form (12), we find that in the resonances in Eq. (6) we have $j_{2\omega} \approx 0$ and the field is

$$E_{2\omega} \approx j_{2\omega}^{(0)} / \sigma_{2\omega}. \quad (13)$$

This means that in integer resonances one should observe an increase of the generation by Ω/ν times, while in the half-integer resonances the singularities in $j_{2\omega}^{(0)}$ and $\sigma_{2\omega}$ cancel each other. Generation bursts are indeed observed in experiment in integer resonances, but not in half-integer ones, thus confirming that the singularities of $j_{2\omega}^{(0)}$ are stronger in integer than in half-integer resonances.

In fact, both the current $j_{2\omega}^{(0)}$ and the conductivity $\sigma_{2\omega}$ contain, besides the resonant terms (11) and (12), also nonresonant terms. In the linear theory it is assumed, e.g., that the large nonresonant contribution to the conductivity is due to glancing electrons and that it is precisely this contribution which is responsible for the small amplitude of the cyclotron resonance in the surface impedance. Glancing electrons contribute, of course, also to the current $j_{2\omega}^{(0)}$ but this contribution can depend only monotonically on the magnetic field. The nonmonotonic structure of the signal in the intervals between the resonances is therefore evidence that the role of the bulk electrons in the formation of the extraneous current is not restricted to the term (11) but contains also another term. It is possible that this second nonlinearity mechanism is due to excitation of cyclotron waves in a metal.¹¹

Obviously, at the integer-resonance (1) points the principal role in $j_{2\omega}^{(0)}$ is played by the resonant term (11). If we compare $j_{2\omega}^{(0)}$ in two integer resonances, we obtain from (11) $j_{2\omega}^{(0)} \propto H_n^{1/2}$. In experiment, the amplitudes of the first two resonances satisfy well the relation $P_{2\omega} \propto H_n$. This can be regarded as an indication that the resonant term in $\sigma_{2\omega}$ is inessential in the region of integer resonances just as in the linear theory.

Far from the integer-resonance points, and in particular near the half-integer resonances, the terms in the current $j_{2\omega}^{(0)}$ may turn out to be of the same order. Since the resonant term varies strongly in the region of the half-integer resonance not only in amplitude but also in phase, the total current $j_{2\omega}^{(0)}$ in fields (2) can, depending on the phase of the nonresonant term, have not only a maximum but also a minimum as well as an intermediate value. In addition, in view of the presence of the nonresonant term in $\sigma_{2\omega}$, the left-hand side of (6) cannot be regarded as equal to zero even at the instant of resonance, and relation (13) is therefore not satisfied. These two circumstances make it impossible to construct a simple qualitative picture for half-integer

resonances (2).

We proceed now to inversion of the resonances. The statement that near integer resonances only the resonant term (11) is of importance in the extraneous current $j_{2\omega}^{(0)}$ is apparently valid only at relatively small H_ω . As seen from Fig. 9, the signal $P_{2\omega}(H)$ in a resonant field saturates relatively rapidly, probably because the inequality (10) is violated. Therefore the minimum of the resonance can be the consequence of interference between the resonant and nonresonant terms in the current $j_{2\omega}^{(0)}$. One cannot exclude, however, also another possibility, namely, that the resonant term (12) in the conductivity $\sigma_{2\omega}$, which has relatively little effect on the impedance, manifests itself in the nonlinear effects much more strongly because of the aforementioned outflow of energy at the frequency 2ω to the resonant system.

The preceding reasoning allows us to construct a qualitative picture that explains the main experimental facts. It appears, however, that it cannot explain the additional structure on the curve, such as, e.g., the broad maximum on the left of the half-integer resonance point. It must be assumed that many details of this structure will find explanation in a more rigorous theory. At the same time, the experimental study of this structure can likewise not be regarded as completed. It is probable that a study of samples with other

orientations will yield additional information concerning this structure. In particular, we are planning to verify whether the minimum X on Figs. 4 and 7 is a manifestation of a resonance of the electrons from the vicinity of the limiting point.

The authors thank A. P. Kopasov and V. T. Dolgoplov for a discussion of the results.

- ¹G. I. Leviev, V. B. Ikonnikov, V. E. Gantmakher, Pis'ma Zh. Eksp. Teor. Fiz. **29**, 634 (1979) [JETP Lett. **29**, 580 (1979)].
- ²A. P. Kopasov, Zh. Eksp. Teor. Fiz. **72**, 191 (1977) [Sov. Phys. JETP **45**, 100 (1977)].
- ³A. P. Kopasov, *ibid.* **78**, 1408 (1980) [**51**, 709 (1980)].
- ⁴A. P. Kopasov and I. A. Mol'kov, 21st All-Union Conf. on Low-Temp. Phys., Abstracts of papers, part III, Khar'kov, 1980, p. 211.
- ⁵V. S. Edel'man, Usp. Fiz. Nauk **123**, 257 (1977) [Sov. Phys. Usp. **20**, 819 (1977)].
- ⁶R. T. Bate and V. R. Visseman, Phys. Rev. **181**, 763 (1969).
- ⁷G. I. Leviev, Zh. Eksp. Teor. Fiz. **62**, 1031 (1972) [Sov. Phys. JETP **35**, 544 (1972)].
- ⁸A. B. Pippard, Rep. Prog. Phys. **23**, 176 (1960).
- ⁹V. T. Dolgoplov, Usp. Fiz. Nauk **130**, 241 (1980) [Sov. Phys. Usp. **23**, 134 (1980)].
- ¹⁰V. Heine, Phys. Rev. **107**, 431 (1957).
- ¹¹E. A. Kaner and V. G. Skobov, Adv. Phys. **17**, 605 (1968).

Translated by J. G. Adashko